ELSEVIER

Ultrasonics Sonochemistry 9 (2002) 297–303

Ultrasonics SONOCHEMISTRY

www.elsevier.com/locate/ultsonch

Surface acoustic cavitation understood via nanosecond electrochemistry. Part III: shear stress in ultrasonic cleaning

Emmanuel Maisonhaute [a], Cesar Prado [b,1], Paul C. White [b,1], Richard G. Compton [b,*,1]

[a] *Département de Chimie, Ecole Normale Supérieure, UMR CNRS 8640 PASTEUR, 24 rue Lhomond, 75231 Paris Cedex 05, France*
[b] *Physical and Theoretical Chemistry Laboratory, Oxford University, South Parks Road, Oxford OX1 3QZ, UK*

Received 27 February 2002; accepted 26 March 2002

Abstract

Acoustic cavitation is extensively used for cleaning purposes. However, little is known about the fundamental aspects of the cleaning process. Our previous electrochemical data suggested that acoustic bubbles were oscillating at a distance of only a few tens of nanometers above the surface [J. Phys. Chem. B 105 (2001) 12087; E. Maisonhaute, B.A. Brookes, R.G. Compton, J. Phys. Chem. B 106 (2002) 3166–3172]. The flow velocities resulting from the bubble collapse lead to important drag and shear forces on the surface, responsible for cleaning and/or eroding the latter. We review here the forces acting on an adsorbed particle located on the surface, and develop arguments to explain why small adsorbates are harder to remove by sonication. Then, experimental results on particle desorption and surface effects brought about by ultrasound are presented and shown to agree with our theoretical predictions.
© 2002 Elsevier Science B.V. All rights reserved.

Keywords: Ultrasound; Cavitation; Shear stress; Bubble; Cleaning; Erosion; Adsorption

1. Introduction

One of the most widespread applications of ultrasound is the cleaning of surfaces [1–11]. This technique is commonly used in most chemistry laboratories, and many effects have been considered in order to explain its efficiency and its limitations. They can be divided into two categories. The first one involves the enhancement of the mass transport via acoustic streaming and microstreaming, which accelerates the dissolution of soluble contaminants. The second implicates mechanical effects happening when cavitation occurs close to a boundary [12–20]. The stresses involved can lead to pitting and are used also to disrupt cells in biological applications. In addition, shock waves, the collision of the bubble wall on the surface upon collapse and microjetting have been considered [21]. For laser induced millimetre bubbles, Lauterborn could quantify the importance of these factors [22]. Observing the rapid growth and disappearance of vapour cavities between two moving surfaces, Israelachvili showed that the nucleation of the cavity can also involve important stresses [23].

Whereas with laser induced bubbles their sizes and positions above the surface can be controlled very precisely, ultrasonic bubbles appear randomly where "cavitation nuclei" are present. These nuclei can be surface inhomogeneities, bubbles remaining from previous cavitation events or impurities [15]. Moreover due to the multiple cavitational events occurring at the same time, the local sound field and acoustic pressures vary with time and are then impossible to control. As a result, it is not possible to predict where and when nucleation will occur. In 1979, Crum showed how to create a millimetre sized bubble on a vibrating plate [24]. Fast scan photographs of this bubble could be taken, showing oscillations in shape and the development of microjet. Most of the mechanical effects were then attributed to the microjet impinging on the surface, albeit often under rather different experimental conditions [25–27]. In fact, the driving frequency was only 60 Hz in Crum's experiment, and to our knowledge no comparable imaging work has been published in the kHz and MHz ranges,

* Corresponding author. Tel.: +33-1-44-32-34-04; fax: +33-1-44-32-33-25.
E-mail addresses: emmanuel.maisonhaute@ens.fr (E. Maisonhaute), richard.compton@chemistry.ox.ac.uk (R.G. Compton).
[1] Tel.: +44-1865-275-448; fax: +44-1865-275-410.

1350-4177/02/$ - see front matter © 2002 Elsevier Science B.V. All rights reserved.
PII: S1350-4177(02)00089-5

where ultrasound finds many applications. In contrast, we recently demonstrated that microjet development was not responsible for the intense and periodic current spikes observed when fast chronoamperometry at microelectrode was carried out [28,29]. An example of chronoamperogram showing 20 kHz oscillation of a single cavitating bubble is given in Fig. 1. In this experiment the current at a microelectrode of diameter 32 μm is measured as a function of time with the electrode potentiostatted at a value corresponding to the transport limited discharge of an electroactive species, in this case the ferricyanide anion in aqueous solution. Full interpretation of electrochemical data revealed that acoustic bubbles were hemispherical rather than spherical, and that their diameter could vary from less than 15 μm up to 0.8 mm in size. The bubble collapse was found to occur at a short distance x_0 of a few tens of nanometers above the surface, and collapse velocities v were found to be in the order of a few hundred meters per second. The chronoamperogram of Fig. 1 can be interpreted as follows: for most of the time, the bubble size is a maximum. The bubble then blocks the electrode, leading to a negligible current. Subsequently, a very fast collapse occurs at distance x_0, and new fresh solution is brought to the electrode surface. A rapid increase of the current is then observed. The bubble then returns to its maximum size, blocking the electrode again and the current drops. Different oscillating frequencies could be observed, corresponding to harmonics or subharmonics of the driving frequency (20 kHz). x_0 was quantified via numerical simulations, and found to vary from 25 nm for very short horn to electrode distances up to 80 nm for larger ones.

The non-zero distance x_0 between the bubble and the surface when the collapse occurs was interpreted considering the force balance on the bubble. On one side, the acoustic pressure P_A "pushes" the bubble towards the collapse, but in opposition to this is the viscosity term σ that "forbids" finite fluid velocities on a surface. The way for the bubble to solve this paradox is to move slightly from the surface to decrease σ. When P_A overcomes σ, a violent collapse occurs. The local acoustic pressure was evaluated in terms of this model via x_0 and v, and found to vary between 25 bars for large electrode to horn distances up to 250 bars for a distance of ≈2 mm. These local and transient acoustic pressures are therefore much higher than the ones measured by calorimetric measurements [30].

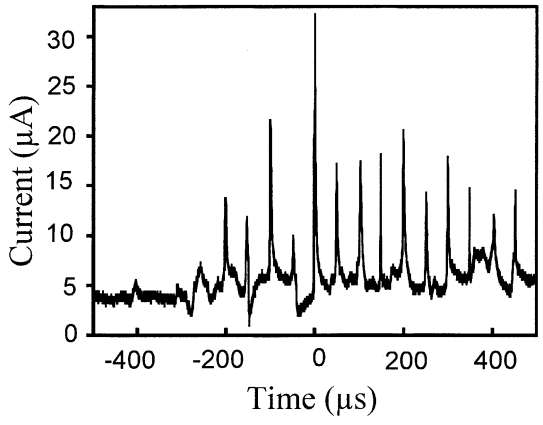

Fig. 1. Single bubble cavitation chronoamperometric current recorded for a 50 mM $K_3Fe(CN)_6$ water solution under sonication at 20 kHz with a 13 mm conical horn, when the electrode potential is held at −0.8 V vs. a Pt pseudo-reference electrode, corresponding to the one electron reduction of $Fe(CN)_6^{3-}$. Electrode to horn distance: 7 mm. Acoustic power: 8.9 W cm^{-2}. Electrode diameter: 32 μm.

Nevertheless, previous papers were aimed only in explaining current shapes and intensities, and we wish to highlight here the conclusions that arise from our electrochemistry experiments for surface cleaning purposes. We report further experiments on the ultrasonic erosion which confirm our understanding of particle removal mechanisms and the surface effects induced by cavitation. We also explain why some molecular adsorbed compounds can not be removed by ultrasound.

2. Experimental

Reagents: $HClO_4$ (Merck) and phenanthrenequinone (Aldrich) were used as received. Aqueous phenanthrenequinone solutions were prepared from stock solutions of phenanthrenequinone in acetone (Aldrich) as described by Anson [31].

Ultrasonic equipment: A 1.3 mm diameter titanium ultrasound horn transducer system (Sonics & Materials, VCX400) calibrated according to a published procedure [30] was used.

Electrodes: The gold microelectrode was home made by sealing a gold wire into soft glass, according to a published procedure [32]. Atomic force microscopy (AFM) electrodes were 3 mm gold wires mounted into Teflon. All electrodes were polished with PRESI papers and then with PRESI 0.3 μm alumina.

AFM: AFM surface imaging of the gold electrode was performed on a NanoScope IIIa system from Digital Instruments, working in contact mode with Nanoprobe SPM Tips (OTR8-35).

3. Forces acting on an adsorbed particle

We give below a few arguments to assist the understanding of the effects of ultrasound on the mechanism of particle removal from a surface. We consider the standard conditions employed using an ultrasonic probe in electroanalysis in which a horn is located "face on" to the electrode. The electrode to horn distance usually ranges between 5 and 10 mm. The ultrasonic power used

in our previous electrochemical experiments was 8.9 $W\,cm^{-2}$. However, the electrochemical response was found to be little affected by an increase of power, probably because of shielding of the sound field by an increased number of bubbles [28].

3.1. Shear forces

Consideration of viscosity requires that the fluid velocity is zero on an insonated surface. Accordingly, a velocity gradient perpendicular to the surface develops. The surface tangential stress σ acting on the surface is given by:

$$\sigma = \eta \mathrm{d}v/\mathrm{d}x \tag{1}$$

where η is the shear viscosity, v the fluid velocity and x the coordinate perpendicular to the surface. For a thin layer of thickness x_0, σ can be approximated as:

$$\sigma \approx \eta v/x_0 \tag{2}$$

v represents the fluid velocity at a distance x_0, resulting from bubble collapse, v has not been measured precisely yet, but it is reasonable to estimate v as being of the order of 200 $m\,s^{-1}$ on the basis of our previous electrochemical experiments [28]. We will take this value as a guideline in the following, but it has to be emphasised that v can be much higher, for example arising from for short electrode to horn distances, and this would lead to stronger effects.

The measured values of x_0 were found to vary approximately from 40 to 80 nm for an electrode to horn distance of 7 mm. Therefore, the local stress on the surface under bubble collapse can be estimated to be $\approx$25 to 50 bars under standard conditions. Note that this stress is estimated considering a steady flow of solution, and thus represents only the minimum stress. The transient behaviour probably induces even higher stresses, but this is presently impossible to quantify.

3.2. Lift forces

According to Saffman [33,34], a gradient in the flow velocity profile induces on a spherical particle of radius R_P a force perpendicular to the flow and equal to:

$$F_L = 6.46 R_P^2 v(\eta\rho \mathrm{d}v/\mathrm{d}x)^{1/2} \tag{3}$$

where R_P is the particle radius and ρ the liquid density.

The associated local pressure P_L is:

$$P_L = 2.056 v(\eta\rho \mathrm{d}v/\mathrm{d}x)^{1/2} \tag{4}$$

In water, for $v = 200$ $m\,s^{-1}$ and $x_0 = 40$ nm, $P_L = 9.2$ bar. The lift force is then smaller than the stress, but since it acts perpendicularly to the surface, it may be able to drag the a particle away from the insonated surface and then to avoid readsorption of the particle if it is detached by the shear stress.

3.3. Drag forces

Considering particles larger than x_0, we consider the velocity profile as being steady state with a velocity v. The drag force acting on these particles may be approximated using Stokes formula:

$$F_D = 6\pi\eta R_P v \tag{5}$$

The values for σ, P_L and F_D have next to be compared to the adhesion force of the particle on the surface. This is described in the next paragraph but it has to be emphasized that when the bubble oscillates periodically on the surface, as the bubble involved in the chronoamperogram of Fig. 1, the cleaning acts several times within a short period and at the same position. This probably enhances the ultrasound cleaning efficiency.

3.4. Attraction force

Different theoretical models allow an estimation of the particle adhesion force to the surface resulting from Van der Waals attraction. They all predict that the force F_{AD} necessary to remove an adsorbed spherical particle from a surface is proportional to its radius R_P. For example, the model elaborated by Johnson et al. provides [35–37]:

$$F_{AD} = -1.5 W_A \pi R_P \tag{6}$$

where W_A is the work of adhesion, which is the sum of the surface energy of the two contacting materials minus the interfacial energy.

Converting this force into a local pressure P_R gives:

$$P_{AD} = -1.5 W_A / R_P \tag{7}$$

The adhesion becomes then much stronger when small particles are adsorbed. Moreover, it has to be emphasized that when molecular size compounds are used specific chemical interaction between the surface and the adsorbate may develop (chemisorption), thus reinforcing the adhesion.

3.5. Force balance

In order to remove a particle, the global removal stress must be stronger than the attractive force.

Considering small adsorbates for which σ is the stronger stress, we take the ratio $\alpha = \sigma/P_{AD}$ as parameter to predict the suitability of ultrasound for removing a particle. From Eqs. (2) and (7) we have:

$$\alpha = \sigma R_P / 1.5 W_A \tag{8}$$

It is difficult to determine which value of α lead to an effective cleaning since other parameters such as time and surface roughness also play an important role [38,39]. Also, a non-spherical adsorbate has a higher adsorption energy than a spherical one, and then needs higher shear stresses to be removed. However, for

polystyrene latex spheres of diameters ranging from 0.1 to 1 μm adsorbed on silicon substrates [40], Busnaina et al. found a 90% removal efficiency for $\alpha = 1$. According to Eq. (8), α decreases with the particle radius to reach very low values for molecular adsorbates. For example, $R_P \approx 1$ nm, $\sigma = 50$ bars and $W_A \approx 1$ J m^{-2} gives $\alpha \approx 0.0033$, which explains why molecular adsorbates are not removed (vide infra). In Section 4, we report experiments that support the theoretical considerations presented above.

4. Experimental results

Below, we discuss previously reported experiments on particle removal first, and then second new experiments on surface erosion.

4.1. Removal of submicrometer particles

This paragraph considers experiments published by Busnaina et al. on the hydrodynamic removal of polystyrene particles adsorbed on silica wafers [4,5,38–50]. For a 0.1 μm diameter particle, the authors give $F_{AD} = 1 \times 10^{-9}$ N, which corresponds to $P_{AD} = 1.3$ bar. Applying Eqs. (5) and (8) with $R_P = 0.05$ μm, $v = 200$ m s^{-1} and $x_0 = 40$ nm leads to $F_D = 1.8 \times 10^{-7}$ N, and $\alpha = 39$.

Thus, ultrasonic cleaning is in principle able to easily remove these particles. In the case of single crystals Si wafers used in semiconductor industry cavitation damage was observed and therefore megasonic cleaning is preferred compared to ultrasonic cleaning because cavitation is reduced. But since megasonic cleaning involves mainly acoustic streaming, the flow velocities achieved are much smaller and then not able to efficiently remove particles of diameters less than 0.1 μm.

4.2. Molecular adsorbates

When small molecules are adsorbed, α quantifies the ultrasound efficiency. However, it was shown in Section 3.5 that α tends to very low values when molecular sizes are reached. It is expected then that cavitation alone is not able to remove these compounds. Instead the increased mass transport may create a faster passivation or surface contamination [51,52]. For example, some of us observed previously that oxidised ascorbic acid was impossible to remove from platinum electrodes by ultrasound [53]. To confirm this analysis, we studied the behaviour under sonication of phenanthrenequinone, a well-documented weakly adsorbed compound. Phenanthrenequinone can be adsorbed at open circuit potential on carbon and gold electrodes from aqueous micromolar solutions [31]. After ≈30 min, a reproducible voltammogram described in Fig. 2 is obtained. The surface coverage obtained by integration of the voltammetric peak of Fig. 2 is 5×10^{-10} mol cm^{-2}. The details of the phenanthrenequinone voltammetry and sonovoltammetry will be described in a separate paper [54]. Desorption under silent conditions takes several hours, which reveal that the desorption rate is activation and not mass transport limited.

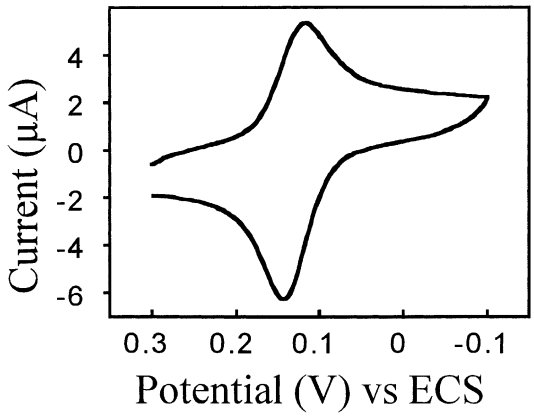

Fig. 2. Voltammogram of an adsorbed film of phenanthrenequinone, in an aqueous solution of 10 μm phenanthrenequinone and 0.1 M $HClO_4$. Scan rate: 100 mV s^{-1}.

After an adsorption time of 30 min, the coated electrode was transposed into a solution containing only the supporting electrolyte. Sonication at a horn to electrode distance of 7 mm was then applied over various period of time ranging from 10 s up to 10 min. The eventual removal of the adsorbate was monitored by integration of the voltammetric peak current. When ultrasound was applied, no modification of the voltammogram was observed. The desorption rate is not accelerated, which proves that ultrasound is inefficient in removing the adsorbed phenanthrenequinone. This is in agreement with the very low values of α achieved for molecular species, and with the fact that the desorption is activation limited. Using shorter horn to electrode distances down to 1 mm did not improve the desorption rate. The only effect was to increase the capacitive current due an increase of area via pitting of the electrode by cavitation, consistently with experiments reported by Madigan [55–58]. We discuss this further in Section 4.3.

Accordingly we suggest that when ultrasound effects are observed with small adsorbates, they should be attributed to a mass transport increase which may enhance dissolution of the adsorbates [2,59] rather than to mechanical cavitation effects. However, as soon as α and then the size reaches some critical value (which depends on the adsorbate size and adsorption energy but also on the sonication power and time and on the electrode to horn distance) ultrasound may be highly beneficial. For example, it has already been observed that ultrasound can prevent polymer growth on an electrode [2], and that it also allows electroanalysis in very "dirty" media, like for example egg samples. In natural samples,

a major drawback for electroanalysis is protein or surfactants adsorption. Since these are large molecules, they are readily removed by sonication, which is then beneficial both for cleaning purposes and increase of mass transport [60,61].

4.3. Effects on surfaces

In this section, we present our investigations carried out on the surface erosion brought about by ultrasound. The samples are first a 60 μm diameter gold microelectrode sealed in glass on which the erosion is detected via optical microscopy and second a 3 mm diameter gold electrode on which we report AFM measurements.

A 60 μm diameter gold electrode was sonicated in pure water at 20 kHz and 8.9 W cm^{-2}. The horn to electrode distance was 2 mm, and after 2 min dramatic effects could be observed. A picture of the electrode taken with a binocular microscope is given in Fig. 3. The electrode surface is no longer smooth, and some cracks in the glass surrounding the electrode can be distinguished (cf. Fig. 3b). After 15 min, strong pitting in the glass was observed (cf. Fig. 3c). The depth of the damage was then ≈200 μm. On the other hand, no effects were observed after 5 min when the horn to electrode distance was 7 mm. Note also that no pitting at all occured for a glass rod sonicated for 5 min at a distance of only 1 mm.

The glass/gold sealing is probably weaker than the glass alone. At short electrode to horn distances, the shear stress produced by the acoustic bubble is strong enough to break the electrode around the sealing. Once a first pit is made, bubbles are preferentially nucleated around this pit. The collapse may also be even stronger when it occurs in a crack. Those two features probably increase the ultrasound effects. The dramatic effects observed for short electrode to horn distances resulting from an important shear stress are consistent with our electrochemical simulations [28] which reveal that the collapse occurs faster and closer to the electrode compared to larger horn to electrode distances, which results in higher σ values (vide supra).

It appears therefore that the bubbles probably appear preferentially at the electrode, which acts as a cavitation nucleus. Previously, we performed probability measurements using a microelectrode array in which several electrodes were sealed in epoxy [29]. The probability of observing the same bubble on two different electrodes was recorded versus the distance. However, whatever the size distribution taken, the obtained probability law was impossible to deconvolute using a model postulating isotropic nucleation, which confirms that bubbles have preferential nucleation sites. Assuming conversely now that bubbles are only nucleated on the electrode, the previously published probability curve would then directly give the size probability. The real behaviour is in truth probably in between these two extremes.

We turn now to AFM measurements. AFM pictures made on polished gold and platinum millimetre electrodes reveal pits and grooves related to the alumina particle size used for polishing [53]. A typical image for a gold electrode polished with 0.3 μm alumina is given in Fig. 4a. Contrasting to what we describe above, no

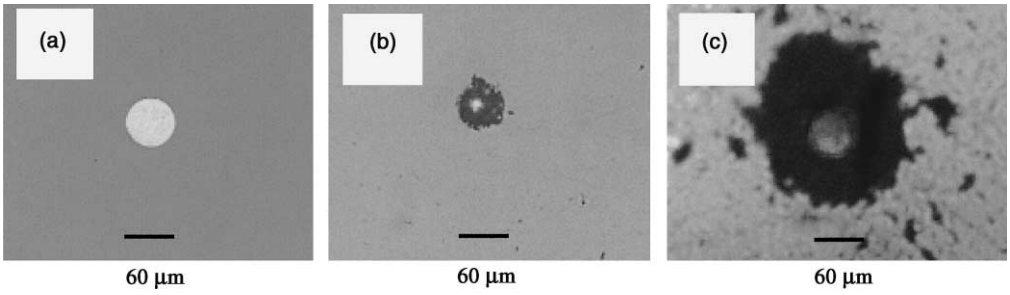

Fig. 3. Optical picture of a 60 μm diameter gold electrode sonicated in water with a power of 8.9 W cm^{-2} and a distance of 2 mm after: (a) 0 min; (b) 2 min and (c) 15 min.

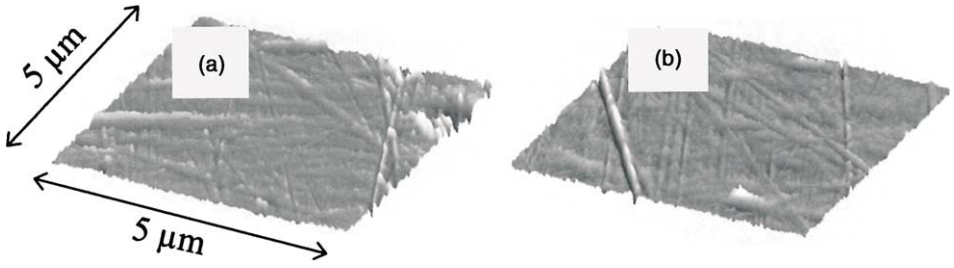

Fig. 4. AFM picture of a 3 mm diameter gold electrode sonicated in water with a power of 8.9 W cm^{-2} and a distance of 2 mm after: (a) 0 min and (b) 2 min.

difference was observed in the AFM picture after sonication for 2 min at 2 mm, over the 5 μm space scale used. For example the polishing lines can still be observed in Fig. 4b. The shear stress does not then seem to affect the electrode at this scale. These observations are consistent with SEM pictures made by Madigan et al. [57]. Then, a smooth gold surface seems at this scale to be hard enough to resist to power ultrasound. However, using a simple binocular loop, it can be seen that the surface roughness has obviously increased. Previously, some of us published AFM pictures of sonicated gold and Pt electrodes on a larger space scale [59,62,63], showing an effective surface modification, consistent with that observed optically as discussed above. The increase of the surface roughness is also apparent when measured electrochemically by ac impedance spectrometry. Ultrasound thus seem to affect the electrode only over a large space scale. This phenomenon is unclear as yet, but has probably to be related to the size of the acoustic bubbles that induce these effects. We previously demonstrated that a wide range of bubble diameters could appear on the surface (up to 0.8 mm diameter bubbles could be detected), and it is likely that the mechanical effects differ with the bubble size. It has also to be underlined that shock waves, not considered in Section 3 because they are not possible to detect electrochemically, may have to be considered in order to explain these large scale effects observed, as suggested by Philipp and Lauterborn [22].

5. Conclusion

Useful information on the complex process underlying the interaction of acoustic bubbles with a surface responsible for the ultrasonic cleaning arises from electrochemical data. Particularly, the shear stress involved during the collapse is suggested to be an important factor. The efficiency of the ultrasonic cleaning strongly depends on the size of the adsorbed particle to be removed and on the electrode to horn distance. Another parameter to take into account may also be the cavitation frequency and the bubble sizes, but no data are presently available for acoustic bubbles nucleated on a surface.

Acknowledgements

We gratefully thank EPSRC for financial support.

References

[1] B. Allard, D.H. McQueen, Ultrasonics (1986).
[2] A. Benahcene, C. Petrier, G. Reverdy, P. Labbe, New J. Chem. 19 (1995) 989.
[3] A.D. Farmer, A.F. Ceilings, G.J. Jameson, Int. J. Miner. Process. 60 (2000) 101.
[4] G.W. Gale, A.A. Busnaina, Part. Sci. Technol. 13 (1995) 197.
[5] G.W. Gale, A.A. Busnaina, Part. Sci. Technol. 17 (1999) 229.
[6] C.R.S. Hagan, S.S. Kher, L.I. Halaoui, R.L. Wells, L.A. Coury, Anal. Chem. 67 (1995) 528.
[7] D.H. McQueen, Ultrasonics 24 (1986) 273.
[8] B. Niemczewski, Ultrason. Sonochem. 6 (1999) 149.
[9] L.G. Olson, J. Sound Vib. 161 (1993) 137.
[10] L.D. Rosenberg, Ultrason. News (1960) 16.
[11] T. Geers, M. Hasheminejad, J. Acoust. Soc. Am. 90 (1991) 3238.
[12] E.L. Cooper, L.A. Coury, J. Electrochem. Soc. 145 (1998) 1994.
[13] B.J. Davidson, N. Riley, J. Sound Vib. 15 (1971) 217.
[14] C.R. Hill, Physical Principles of Medical Ultrasonics, Ellis Horwood, 1986.
[15] T.G. Leighton, The Acoustic Bubble, Academic Press, 1994.
[16] T.J. Mason, Chem. Br. 22 (1986) 661.
[17] W.L. Nyborg, J. Acoust. Soc. Am. (1958) 329.
[18] S.A. Perusich, R.C. Alkire, J. Electrochem. Soc. 138 (1991) 700.
[19] S.A. Perusich, R.C. Alkire, J. Electrochem. Soc. 138 (1991) 708.
[20] A.R. Williams, Ultrasound: Biological Effects and Potential Hazards, Academic Press, New York, 1983.
[21] M.S. Plesset, R.B. Chapman, J. Fluid Mech. 47 (1971) 283.
[22] A. Philipp, W. Lauterborn, J. Fluid Mech. 361 (1998) 75.
[23] L.C. You, T. Kuhl, J. Isralachvili, Wear 153 (1992) 31.
[24] L.A. Crum, J. de Phys. 11 (1979) C8.
[25] P.R. Birkin, S. SilvaMartinez, J. Electroanal. Chem. 416 (1996) 127.
[26] P.R. Birkin, S. SilvaMartinez, Anal. Chem. 69 (1997) 2055.
[27] P.R. Birkin, C.L. Delaplace, C.R. Bowen, J. Phys. Chem. B 102 (1998) 10885.
[28] E. Maisonhaute, B.A. Brookes, R.G. Compton, J. Phys. Chem. B 106 (2002) 3166–3172.
[29] E. Maisonhaute, P.C. White, R.G. Compton, J. Phys. Chem. B 105 (2001) 12087–12091.
[30] M.A. Margulis, A.N. Maltsev, Russ. J. Phys. Chem. 43 (1969) 592.
[31] A.P. Brown, F.C. Anson, Anal. Chem. 47 (1977) 1589.
[32] R.M. Wightman, D.O. Wipf, Electroanal. Chem. 15 (1989) 267.
[33] P.G. Saffman, J. Fluid Mech. 22 (1965) 385.
[34] M.A. Rizk, S.E. Elghobashi, Phys. Fluid 28 (1985) 806.
[35] K.L. Johnson, K. Kendall, A.D. Roberts, Proc. R. Soc. London A 324 (1971) 301.
[36] B.V. Derjaguin, Kolloid Z. 69 (1934) 155.
[37] V.M. Muller, V.S. Yuschenko, B.V. Derjaguin, J. Colloid. Interface Sci. 77 (1980) 91.
[38] A.A. Busnaina, Kashkoush II, G.W. Gale, J. Electrochem. Soc. 142 (1995) 2812.
[39] A.A. Busnaina, G.W. Gale, Part. Sci. Technol. 15 (1997) 361.
[40] A.A. Busnaina, J. Taylor, I. Kashkoush, J. Adhes. Sci. Technol. 7 (1993) 441.
[41] A.A. Busnaina, T.M. Elsawy, J. Electron. Mater. 27 (1998) 1095.
[42] A.A. Busnaina, F. Dai, J. Adhes. 67 (1998) 181.
[43] A.A. Busnaina, T. Elsawy, J. Adhes. 74 (2000) 391.
[44] S. Krishnan, A.A. Busnaina, D.S. Rimai, L.P. Demejo, J. Adhes. Sci. Technol. 8 (1994) 1357.
[45] D.S. Rimai, A.A. Busnaina, Part. Sci. Technol. 13 (1995) 249.
[46] D.S. Rimai, D.J. Quesnel, A.A. Busnaina, Colloid. Surf. A—Physicochem. Eng. Asp. 165 (2000) 3.
[47] Suni II, G.W. Gale, A.A. Busnaina, J. Electrochem. Soc. 146 (1999) 3522.
[48] J. Tang, A.A. Busnaina, J. Adhes. 74 (2000) 411.
[49] F. Zhang, A.A. Busnaina, G. Ahmadi, J. Electrochem. Soc. 146 (1999) 2665.
[50] F. Zhang, A.A. Busnaina, M.A. Fury, S.Q. Wang, J. Electron. Mater. 29 (2000) 199.
[51] R.G. Compton, F. Marken, T.O. Rebbitt, Chem. Commun. (1996) 1017.

[52] F. Marken, R.P. Akkermans, R.G. Compton, J. Electroanal. Chem. 415 (1996) 55.
[53] R.P. Akkermans, M. Wu, C.D. Bain, M. Fidel-Suarez, R.G. Compton, Electroanalysis 10 (1998) 613.
[54] E. Maisonhaute, R.G. Compton, J. Electroanal. Chem. (2001).
[55] N.A. Madigan, C.R.S. Hagan, L.A. Coury, J. Electrochem. Soc. 141 (1994) L23.
[56] N.A. Madigan, T.J. Murphy, J.M. Fortune, C.R.S. Hagan, L.A. Coury, Anal. Chem. 67 (1995) 2781.
[57] N.A. Madigan, C.R.S. Hagan, H.H. Zhang, L.A. Coury, Ultrason. Sonochem. 3 (1996) S239.
[58] N.A. Madigan, L.A. Coury, Anal. Chem. 69 (1997) 5.
[59] R.G. Compton, J.C. Eklund, S.D. Page, G.H.W. Sanders, J. Booth, J. Phys. Chem. 98 (1994) 12410.
[60] J. Davis, R.G. Compton, Anal. Chim. Acta 404 (2000) 241.
[61] E.L. Beckett, N.S. Lawrence, Y.C. Tsai, J. Davis, R.G. Compton, J. Pharm. Biomed. Anal. 26 (2001) 995–1001.
[62] R.G. Compton, J.C. Eklund, F. Marken, T.O. Rebbitt, R.P. Akkermans, D.N. Waller, Electrochim. Acta 42 (1997) 2919.
[63] F. Marken, S. Kumbhat, G.H.W. Sanders, R.G. Compton, J. Electroanal. Chem. 414 (1996) 95.